



**HAL**  
open science

## Renewable phosphorous-based flame retardant for lignocellulosic fibers

Karina Antoun, Melek Ayadi, Roland El Hage, Michel Nakhl, Rodolphe  
Sonnier, Carole Gardiennet, Nicolas Le Moigne, Arnaud Besserer, Nicolas  
Brosse

► **To cite this version:**

Karina Antoun, Melek Ayadi, Roland El Hage, Michel Nakhl, Rodolphe Sonnier, et al.. Renewable phosphorous-based flame retardant for lignocellulosic fibers. *Industrial Crops and Products*, 2022, 186, pp.115265. 10.1016/j.indcrop.2022.115265 . hal-03708784

**HAL Id: hal-03708784**

**<https://imt-mines-ales.hal.science/hal-03708784>**

Submitted on 30 Jun 2022

**HAL** is a multi-disciplinary open access archive for the deposit and dissemination of scientific research documents, whether they are published or not. The documents may come from teaching and research institutions in France or abroad, or from public or private research centers.

L'archive ouverte pluridisciplinaire **HAL**, est destinée au dépôt et à la diffusion de documents scientifiques de niveau recherche, publiés ou non, émanant des établissements d'enseignement et de recherche français ou étrangers, des laboratoires publics ou privés.

# Renewable phosphorous-based flame retardant for lignocellulosic fibers

Karina Antoun<sup>a,b</sup>, Melek Ayadi<sup>a</sup>, Roland El Hage<sup>b</sup>, Michel Nakhl<sup>b</sup>, Rodolphe Sonnier<sup>c</sup>, Carole Gardienet<sup>d</sup>, Nicolas Le Moigne<sup>c</sup>, Arnaud Besserer<sup>a</sup>, Nicolas Brosse<sup>a,\*</sup>

<sup>a</sup> Laboratoire d'Etude et de Recherche sur le MATériau Bois (LERMAB), Faculté des Sciences et Technologies, Université de Lorraine, Bld des Aiguillettes, Vandœuvre-lès-Nancy F-54500, France

<sup>b</sup> Laboratoire de Chimie Physique des Matériaux (LCPM), EDST-PR2N, Faculté des Sciences II, Université Libanaise, Fanar, Lebanon

<sup>c</sup> Polymers Composites and Hybrids (PCH), IMT Mines Ales, Ales, France

<sup>d</sup> Laboratoire de Cristallographie, Résonance Magnétique et Modélisations (CRM2), UMR 7036 CNRS, Université de Lorraine, Faculté des Sciences et Technologies, Nancy, France

## A B S T R A C T

An easy-to-use and environmentally friendly method is proposed to increase the fire retardancy of natural fibers. Hemp fibers were phosphorylated by the grafting of phytic acid, a renewable and environmentally friendly phosphorous flame retardant and urea in aqueous solution. The fibers were characterized by X-ray fluorescence, solid state <sup>13</sup>C and <sup>31</sup>P NMR analysis, pyrolysis combustion flow calorimetry and tensile testing. The swelling behavior of the fibers evaluated by optical microscopy observations showed that urea promotes swelling and consequently the grafting of P and N in the fiber. It has been also shown by a bleaching step that delignification makes the cellulose slightly more accessible for grafting. Non-flammable fibers were produced with relatively low P and N contents (> 0.5 % w/w and > 0.7 % w/w respectively). However, the phosphorylation process significantly decreased cellulose crystallinity and mechanical properties of the resulting fibers. For P = 0.9 %, a 30 % decrease in the tensile strength of hemp fibers was observed. The production of phytic pyrophosphate by thermal dehydration of phytic acid has been proposed from <sup>31</sup>P NMR results.

### Keywords:

Natural fiber

Hemp fiber

Flame retardant

Phytic acid

## 1. Introduction

In recent years, research and innovation in lignocellulosic materials have grown rapidly. This interest is justified by the benefits of these materials over others, including their low cost, low density, low environmental impact, biodegradability and potential use in a wide range of applications. However, the high flammability of these materials remains a limitation that hinders their broad development. To tackle such drawback, reinforcement or modification of the chemical structure of lignocellulosic materials with a flame retardant agent can be considered. Flame retardant can be divided into two types based on their composition: halogenated, which have been used extensively in the past and non-halogenated (Costes et al., 2017; Li et al., 2021; Sykam et al., 2021). Due to both environmental and health concerns, there are increasing efforts to avoid the use of halogenated flame retardants (Li et al., 2021; Morgan et al., 2013). As an alternative to these, phosphorous flame retardants are increasingly used for lignocellulosic materials due their effectiveness in flame retardancy performance (Hajj et al., 2018, 2020; Sonnier et al., 2015). Their action mechanism at high temperature

involves a phosphorylation reaction of cellulose, which inhibits the formation of flammable levoglucosan, and consequently reduces the fuel supply necessary for maintaining the flame.

In our recent work, an efficient and inexpensive process has been developed to improve the fire retardancy of hemp fibers. This process consists in an impregnation of hemp fibers in an aqueous solution of etidronic acid and urea followed by a cooking step. This reaction is based on an old and well-known phosphorylation method for cellulose or starch performed at the solid state (Passauer et al., 2017). It has been shown that the thermal properties of modified hemp fibers have been considerably improved by the synergic effect of N and P (Moussa et al., 2020). However, etidronic acid is a synthetic molecule and there is a strong need for the use of renewable and environmentally friendly phosphorous flame retardant.

At the end of the 19th century, phytic acid (PA, inositol-hexaphosphoric acid) has been identified in seeds. During the development and maturation phase of seeds, phytin accumulates (Lott et al., 1995). As a result, in mature seeds PA represents about 70 % of total phosphorous content in legumes, grains, nuts and oilseeds

\* Corresponding author.

E-mail address: nicolas.brosse@univ-lorraine.fr (N. Brosse).

(García-Esteba et al., 1999). PA promotes growth during the early stages of germination and seed establishment (Mandizvo and Odindo, 2019) and is also known as one of the major antinutrients present in cereals because of its ability to act as a chelator of micronutrients (Alkandari et al., 2021; García-Esteba et al., 1999; Hurrell et al., 2003). In literature PA has been used for flame retardancy through its high phosphorous content (Zhao et al., 2021). PA was first used in combination with chitosan as a coating treatment on cotton fabrics. There was a clear improvement in the fire performance of coated fabrics containing a high amount of phytic acid comparing to those coated with a high chitosan content material (Laufer et al., 2012). PA was also used for wood as flame retardant. The wood sample was impregnated in a PA solution to allow the PA molecules to penetrate the wood textures. After treatment, the wood sample showed excellent flame retardancy (Wang et al., 2022). Ammonium phytate has been described to improve the flame resistance of "Lyocell" fibers through a grafting in the presence of dicyanamide in water. Results demonstrate that modified lyocell fibers displayed excellent durable fire- retardancy performances (Liu et al., 2018).

The objective of this work is to propose an environmentally friendly and industrializable process for the fire retardancy of cellulosic fibers. A water-based and easy scalable treatment process was proposed using PA and urea by covalent grafting of phytate moiety. The optimization of the different process parameters and the importance of the reagents has been examined. The thermal decomposition of grafted hemp fibers was studied by pyrolysis combustion flow calorimeter. The phosphorous content was determined by Inductively coupled plasma and X-ray fluorescence, and the fixation of phosphate groups was evaluated by  $^{31}\text{P}$  and  $^{13}\text{C}$  solid state NMR spectroscopy. The impact of the treatment on the swelling and the mechanical strength of the fiber was also analyzed.

## 2. Materials and Methods

### 2.1. Raw materials

In this study, hemp fibers were provided by "La Chanvrière, Bar sur Aube, France" company. Phytic acid, urea, sodium hydroxide, glacial acetic acid, sodium chlorite, dichloromethane, and sulfuric acid were purchased from Sigma Aldrich Company (St. Quentin Fallavier, France). The hemp fibers used in this study have first undergone a steam explosion refining step after a soda impregnation (NaOH, 8 % w/w) according to a previously described process (Sauvageon et al., 2018). The optimal parameters used based on a previous study, to produce exploded fibers composed of 91 % of elementary fibers were as follows: temperature = 190 °C; time = 4 min (Sauvageon et al., 2018). The chemical composition of hems fibers used in this study is given in Table 1. After pre-treatment, most of the hemicelluloses were extracted, leading to a decrease in hemicellulose content. This reduction is due to extensive hydrolysis of non-cellulosic polysaccharides during the steam explosion process (Ziegler-Devin et al., 2021).

### 2.2. Bleaching process

Bleached fibers were obtained using a delignification treatment based on acetic acid and sodium chlorite. Exploded fibers were placed in

**Table 1**  
Chemical composition of hemp fibers.

Fibers	Chemical composition			
	Extractives	Lignin	Hemicelluloses	Cellulose
RHF <sup>a</sup>	5.8 ± 0.8	4.6 ± 0.6	11.3 ± 2.3	53.1 ± 1.3
HF <sup>b</sup>	4.9 ± 0.1	3.1 ± 0.2	1.5 ± 0.2	79.4 ± 7.6
BHF <sup>c</sup>	11.3 ± 2	2.6 ± 0.6	1.2 ± 0.2	73.6 ± 6.9

<sup>a</sup> Raw hemp fiber.

<sup>b</sup> Exploded hemp fiber.

<sup>c</sup> Bleached exploded hemp fiber

a double jacketed glass reactor with deionized water (83.3 mL/g fiber), sodium chlorite (0.67 g/g fiber) and glacial acetic acid (0.67 mL/g fiber). The mixture was heated at 70 °C for 6 h, then a whitish solid residue consisting mainly of holocellulose was obtained. After cooling, the bleached fibers were filtered under vacuum and washed extensively with deionized water until neutral pH. The bleached exploded hemp fibers were dried overnight at room temperature before being used.

### 2.3. Grafting process

The exploded hemp fibers (HF) and bleached exploded hemp fibers (BHF) were phosphorylated using various experimental conditions (Table 2). Fibers were first impregnated in an aqueous solution of urea (8–20 wt%) and phytic acid (3–7 wt%). A quantity of 10 g of HF and BHF is impregnated in 100 mL of each of the 7 aqueous solutions of PA and urea. This impregnation is carried out for 1 h without stirring at room temperature. The impregnated fibers were filter-pressed to remove free-water before they were dried in an oven at 60 °C overnight to reach a 20 wt% of relative humidity. The grafting of the HF and HFB was achieved by a cooking step at a temperature of 150 °C for 2 h. At the end of the treatment, the phosphorylated fibers were washed thoroughly 5 times with distilled water and then filtrated under vacuum before being dried under a hood for 48 h.

### 2.4. Characterization techniques

#### 2.4.1. Elemental analysis

For the elemental analysis of carbon, nitrogen, oxygen and hydrogen, a "Thermo Finnigan Flash EA 112 Series" was used. The combustion of the samples (1.5 mg) to be analyzed is performed at high temperature (1,000 °C) for 15 s in the presence of tungstic anhydride, under oxidizing atmosphere. This decomposition gives H<sub>2</sub>O, CO<sub>2</sub>, SO<sub>2</sub>, NO<sub>x</sub> which is reduced to N<sub>2</sub> in the presence of copper. These gaseous products are then analyzed by gas chromatography. The results are recorded and analyzed by the software "Eager 300" which calculates directly the percentage of each element present in the compound.

#### 2.4.2. X-ray fluorescence (XRF)

was used as a non-destructive technique to identify the phosphorous content. It is based on counting of fluorescent X-rays emitted by a sample after being excited by a primary X-ray source. In every sample, each element produces specific fluorescent X-rays. The analyses were carried out under atmospheric pressure, without any preparation. The fiber was irradiated with x-rays and each spectrum was collected for 8 min. As the intensity of the phosphorous peak is proportional to its concentration, data were collected and converted by a simple calculation to determine the mass percentage of phosphorous. Each sample was analyzed 3 times to ensure reproducibility of the measurements.

#### 2.4.3. Solid state NMR analysis

Previously milled hemp fibers were compressed in a 4-mm diameter zirconium oxide NMR rotor. Solid-state NMR experiments were carried out on a Bruker Biospin AVANCE III spectrometer operating at a magnetic field of 14 T corresponding to a  $^1\text{H}$  resonance frequency of 600 MHz. The spinning frequency was set to 9 kHz. All spectra were acquired without temperature regulation. TMS and H<sub>3</sub>PO<sub>4</sub> were used as external  $^{13}\text{C}$  and  $^{31}\text{P}$  chemical shift references. During  $^{31}\text{P}$  direct acquisition spectra, the  $^{31}\text{P}$  90 ° pulse length was set to 6 μs.  $^{31}\text{P}$  longitudinal relaxation times (T<sub>1</sub>) were measured (data not shown) and a 50 s recycle delay, which is at least 5 times longer than the highest T<sub>1</sub>, was chosen to ensure quantitative measurements. 80 kHz SPINAL-64  $^1\text{H}$  decoupling was applied during 20 ms acquisition (Fung et al., 2000).  $^{13}\text{C}$  cross-polarization spectra were recorded with  $^1\text{H}$  and  $^{13}\text{C}$  fields of 57 kHz and 48 kHz, respectively, applied during a 1 ms contact time. 70 kHz SPINAL-64  $^1\text{H}$  decoupling was applied during 20 ms acquisition (Fung et al., 2000). The recycle delay was 3 s. Spectra were processed

**Table 2**

Main data for phosphorylated hemp fibers.

Sample ref	Bleaching	Urea% <sup>a</sup>	PA% <sup>b</sup>	P% <sup>c</sup>	N% <sup>d</sup>	PCFC				
						pHRR (W/g)	TpHRR (°C)	THR (kJ/g)	ΔH (kJ/g)	Residu (%)
1	No	–	–	–	–	300.8	358.6	12.4	13,3	7
2	Yes	–	–	–	–	312.0	351.6	12.7	13,4	5
3	No	1	0.32	0.15	0.05	260.9	322.0	11.1	12,1	8
4	Yes	1	0.32	0.12	0.28	152.1	292.9	8.30	9,9	16
5	No	2	0.63	0.24	0.31	180.4	295.9	8.90	10,1	12
6	Yes	2	0.63	0.33	0.48	108.2	276.5	6.70	8,6	22
7	No	5	1.57	0.53	0.66	85.30	266.1	5.40	7,2	25
8	Yes	5	1.57	0.66	0.85	83.75	262.3	4.90	6,4	24
9	No	10	3.13	0.93	0.78	57.80	255.9	3.40	4,8	29
10	Yes	10	3.13	1.53	1.26	50.00	247.0	2.90	4,4	35
11	No	15	4.70	1.48	1.07	46.30	250.5	2.50	3,9	36
12	Yes	15	4.70	1.97	1.42	41.26	241.8	2.10	3,2	35
13	No	20	6.26	1.83	1.40	42.90	237.6	2.30	3,5	34
14	Yes	20	6.26	2.40	1.48	39.20	238.4	1.70	2,7	36
15	No	20	–	–	0.54	265.0	348.0	12.8	13,2	3
16	No	–	6.26	1.10	–	72.00	254.5	3.40	4,8	29
17 <sup>e</sup>	No	20	6.26	0.10	0.05	193.0	305.0	8.50	9,1	6

<sup>a</sup> urea in wt% in the impregnation solution;<sup>b</sup> PA in wt% in the impregnation solution;<sup>c</sup> determined by ICP;<sup>d</sup> determined by centesimal composition;<sup>e</sup> cooking time = 0 hr.

and plotted with ssNake (Van Meerten et al., 2019). Deconvolutions were performed with DMFIT software (Massiot et al., 2002).

#### 2.4.4. Pyrolysis combustion flow calorimetry (PCFC)

Fire behavior of samples at microscale (2–4 mg) was investigated using a pyrolysis combustion flow calorimeter (Fire Testing Technology Ltd., UK). The samples were pyrolyzed with a temperature rise rate of 1 °C/sec under a nitrogen flow (100 mL/min) from 90 °C to 750 °C (anaerobic pyrolysis). The pyrolysis gases were transported to a combustor in the presence of a N<sub>2</sub>/O<sub>2</sub> (80/20) mixture. Under such conditions, all gases are fully oxidized. Heat release rate (HRR) was calculated according to the Huggett relation (Huggett et al., 1980). According to this relation, 1 Kg of oxygen consumed corresponds to 13.1 MJ of heat release. Each sample was tested twice to ensure reproducibility of the measurements. The peak heat release (pHRR), temperature at pHRR (TpHRR), total heat release (THR), heat of combustion (ΔH), and final residue rate (%) were determined. In order to highlight the influence of phosphorous on the char stability, the solid residues obtained with anaerobic pyrolysis were studied using aerobic pyrolysis. Heating rate, maximum pyrolysis temperature, combustion temperature and gas flow rate were respectively 1 °C.s<sup>-1</sup>, 750 °C, 900 °C (corresponding to complete combustion) and 100 cm<sup>3</sup>.min<sup>-1</sup>. Oxygen was introduced at various fractions (0.01, 0.02, 0.05, 0.1 and 0.2) into the pyrolyzer to measure the thermo-oxidative stability of the char. When low oxygen fractions are chosen for aerobic pyrolysis, oxygen may be fully consumed and the combustion may become incomplete. To avoid this issue, 1 mg-sample was tested.

#### 2.4.5. Preliminary fire test on fibers

An unstandardized fire test was performed to evaluate the flammability of the fibers in a simple and quick way. Raw and treated fibers previously glued vertically on an aluminum support are ignited by a lighter. This method allows the fibers self-extinguishment to be evaluated, i.e. absence of flame spreading. Three behaviors are thus discriminated: flame propagation without stable residue, flame propagation with stable residue and no flame propagation (self-extinguishing), and no flame take (non-flammable). The residue is also weighed after complete burning. The initial mass of each fiber is subtracted from the mass of the residue to calculate the percentage of mass loss (% residue).

#### 2.4.6. Optical microscopy

Fiber swelling was studied on fibers impregnated with water, PA solution and a mixture urea/PA. Swelling experiments were carried out with a Laborlux 12 Pol S optical microscope in transmission mode (Leica, Wetzlar, Germany) equipped with a mono-CDD Sony digital camera (resolution 1,600 × 1,200 pixels, Tokyo, Japan) and an image acquisition software Archimed® (Microvision Instruments, Lisses, France). The fibers were placed between two glass plates and their diameter was measured before and after the addition of water, PA and urea/PA solutions injected by capillarity using a pipette. To ensure reproducibility of measurements, each type of fiber sample was analyzed 10 times and 20 diameter values were taken along each fiber before and after impregnation.

#### 2.4.7. Mechanical properties

The measurements of the fibers mechanical properties were carried out using a Favimat Robot (Textechno Herbert Stein GmbH and Co. KG, Möchengladbach, Germany). The displacement is ensured by a constant speed motor (5 mm/min) and the fiber is clamped between two sets of jaws before starting the test. The load and elongation data were analyzed and plotted, and the percentage of elongation and breaking point were determined with reference to NF EN ISO 5079 1996 Standard method Textiles. The tensile strength was calculated in function of the surface of fiber which was determined by Scanning Electron Microscopy. The fibers were manually separated and parallelized. They were then introduced in the sample holder in the Scanning Electron Microscope (Hitachi TM3000). The images were taken at an acceleration voltage of 15 kV. X 300 magnification was used to give a representative image of the overall fibrous structure whereas X 1,000 magnification was used to more closely examine individual fiber cross section.

### 3. Results and discussion

In this study, the phosphorylation of hemp fiber (HF) was carried out using a commercial phytic acid-rich crude extract (PA). The water-based phosphorylation process was adapted from our previously described method carried out with urea and etidronic acid (Moussa et al., 2020). Increasing concentrations of reagents in the impregnation solution have been tested until 20 wt% and 6.26 wt% for urea and PA respectively using HF and BHF. The phosphorous and nitrogen contents, the PCFC and preliminary fire test results are gathered in Table 2 (essay 1–14) and

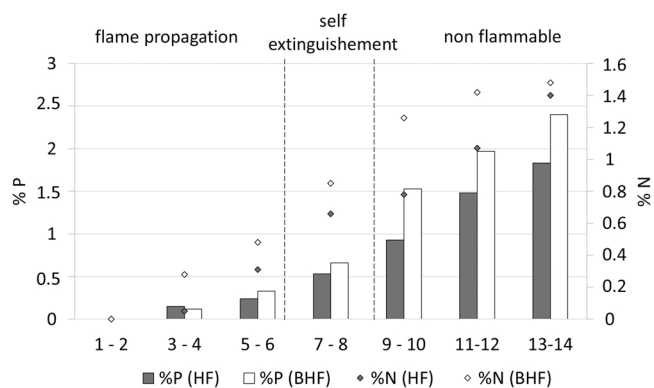


**Fig. 1.** The variation of the P and N rate as a function of PA-urea solution and its effect on the combustion of fibers.

in Figs. 1 and 2. All the analysis given in Table 2 were performed after an extensive washing of the fibers (see Materials and Methods section). P% was determined par XRF analysis directly on the fibers (non-destructive method). In a preliminary study given in Supplementary Materials (SM1), a comparative study carried out with inductively coupled plasma atoms emission spectroscopy (ICP-AES) after mineralization revealed small deviations between XRF and ICP-AES. It was observed that, like etidronic acid (Moussa et al., 2018), the grafting of PA on the fiber is achieved in the presence of urea and that P% and N% increased with the reagent's concentrations.

As seen in Fig. 1, at low P% ( $< 0.2$  wt%), the fibers ignited and burned (essays 3–6). For  $P \approx 0.5$  wt%, the fiber became self-extinguishing (essays 7, 8) and for  $P > 0.5$  wt% the fibers were totally non-flammable (essays 9–14). It was also observed in Fig. 1 that P and N contents were slightly higher for the BHF compared with lignified HF. These observations indicate that delignification makes cellulose more accessible for phosphorous and nitrogen grafting.

Fig. 2 gives the HRR curves for HF (A) and BHF (B). The phosphorylation of hemp fibers using urea/PA led to a reduction in thermal stability, pHRR, THR and to an increase in char content. As the percentage of P and N grafted onto the hemp fibers increased, the pHRR decreased while shifting to a lower temperature. The pHRR decreased from  $\approx 300$  W/g (essay 1–2, P, N = 0 wt%) to  $\approx 40$  W/g (essay 13–14, P  $\approx 2$  wt%, N  $\approx 1.5$  wt%). The temperature of the pHRR decreased from  $358.6$  °C for the non-treated fiber (essay 1) to  $237.6$  °C for the fiber treated and grafted with 1.83 wt% of P (essay 13). The total heat release (THR) decreased also when the phosphorous content increased from

12.4 KJ/g (essay 1) to less than 2.3 KJ/g when the fibers are grafted with 1.83 wt% of P (essay 13).

These results showed that phosphorylation not only improved carbonization, but also changed the composition of the released gases. Indeed, the char being rich in carbon, an increase of the char content with P wt% (as shown in Table 2) implied the formation of less carbon-rich gases.

A solution containing 10 wt% of urea and 3.13 wt% of phytic acid (essay 9, P  $\approx 0.93$  wt%, N  $\approx 0.78$  wt%) was sufficient for a good fire performance. The same trend was observed for BHF where the pHRR temperature decreased to  $250$  °C when P reaches 1.5 wt%. The pHRR, THR and heat of combustion decreased also when the phosphorous content increased. This decrease is associated with an increase in the char rate (about 30 %), thus, char formation is pomoted and less combustibile reactive species are released.

All these observations are in accordance with previous studies dealing with natural fibers modified with phosphorous flame retardants (Coleman et al., 2011; Wan et al., 2020), phosphorylation resulting in a reduction in thermal stability, pHRR, THR and  $\Delta H$  and an increase in char content. A comparison between phosphorylated flax fibers (Sonnier et al., 2015; Hajj et al., 2018), hemp fibers (Moussa et al., 2020) and this study, is presented in Fig. 3. The pHRR decreased similarly for all fibers when phosphorous content increased and the same behavior was also observed for the THR. This observation indicates that flame retardancy at microscale appears to depend solely on phosphorous content, regardless of the nature of the phosphorylating agent.

During combustion, the residue can act as a protective insulating layer. Pyrolysis is considered anaerobic as long as the flame is maintained. When the flame fades, the residue can be subjected to aerobic pyrolysis. The char residues obtained using direct anaerobic pyrolysis of phosphorylated fibers with various levels of phosphorous were studied in PCFC using aerobic pyrolysis. The comparison of char residues using aerobic pyrolysis with 20 %  $O_2$  showed that the temperature ( $T_{pHRR}$ ) increased from  $389.8$  °C for untreated fibers (0.07 wt% P) to  $509.6$  °C for treated fibers with 1.8 wt% P (Fig. 4-A). The influence of phosphorous on the thermo-oxidative stability is well clear, it appears that a low phosphorous content is enough to slightly improve the thermo-oxidative stability. A higher phosphorous content no longer improved the thermo-oxidative stability but increased the carbon content (Chapple et Anandjiwala, 2010). Fig. 4B showed the change of pHRR temperature versus the oxygen fraction in the case of a char prepared from treated hemp fiber (sample 9). The analyses were carried out for five oxygen fractions: 0.01; 0.02; 0.05; 0.1 and 0.2. The temperature of pHRR decreased as the oxygen fraction increased, thus, the decomposition rate increased as the oxygen fraction increased. Char residues of BHF has

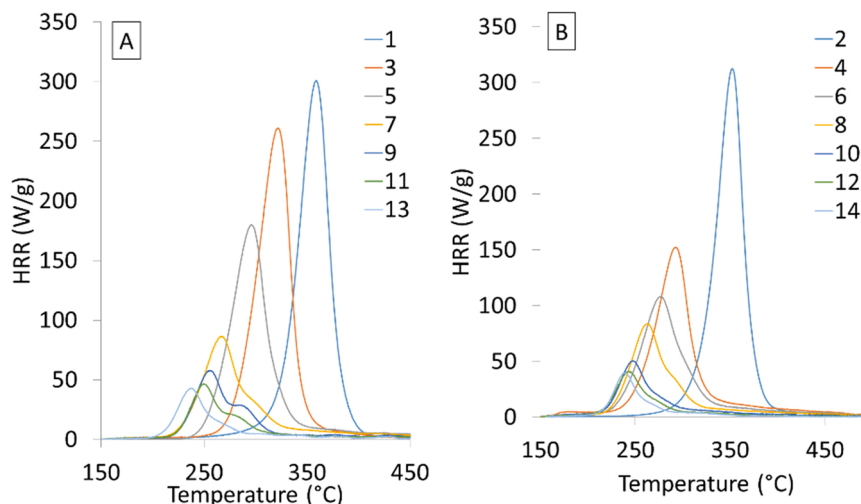


**Fig. 2.** HRR curves at PCFC (A) for HF and (B) for BHF with various levels of phosphorylation.



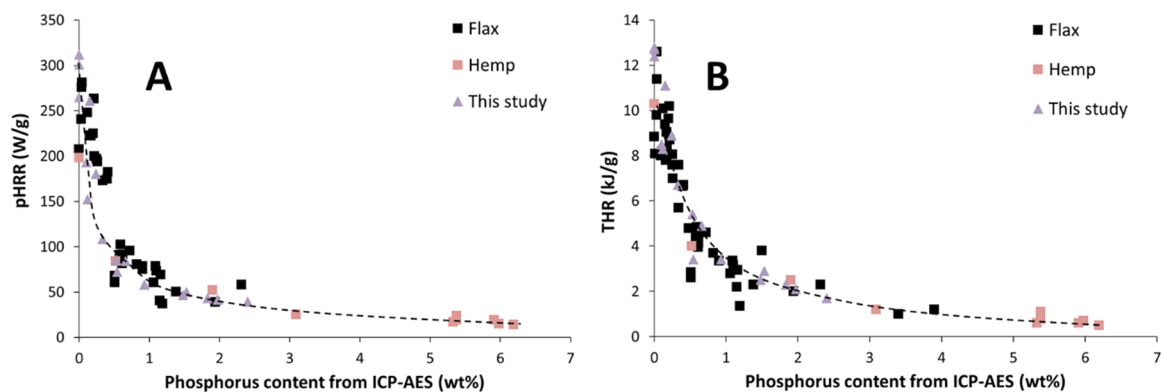


Fig. 3. pHRR and THR versus phosphorous content for modified flax and hemp fibers (data for flax can be found in [Sonnier et al., \(2015\)](#); [Hajj et al., \(2018\)](#); and for hemp fiber [Moussa et al., \(2020\)](#)).

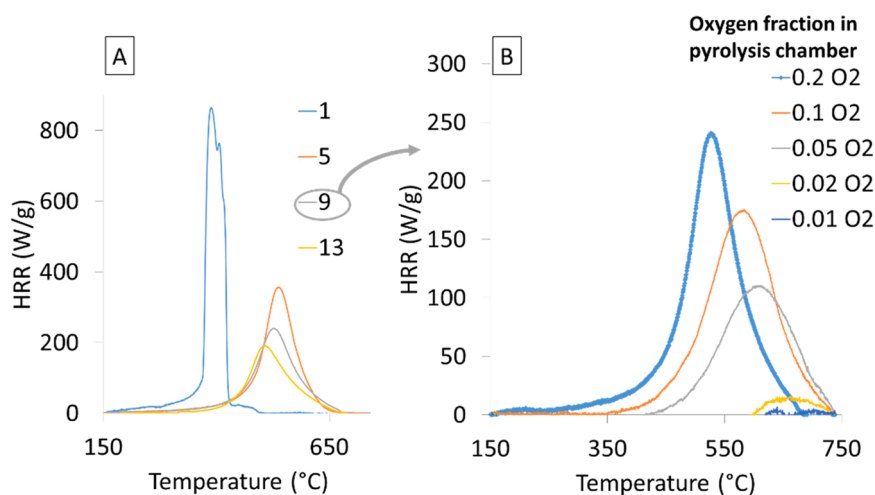


Fig. 4. HRR curves for char prepared from fibers (1, 5, 9 and 13) aerobic pyrolysis (A) using 20 % O<sub>2</sub> and (B) char of fiber (9) using various oxygen fractions.

been also studied by aerobic pyrolysis ([Supplementary Materials, SM2](#)). Results clearly showed that thermo-oxidative stability was improved with the increase of P wt%.

An optimization of the grafting conditions (cooking and impregnation time) has been carried out on HF and BHF. The percentage of urea and phytic acid in the aqueous solution was fixed at 10 wt% and 3.13 wt % respectively (essay 9 conditions). The results presented in [Supplementary Materials \(SM3 to SM6\)](#) showed that a cooking time of 20 min was sufficient while an impregnation time of one hour is required for better fire performance.

In order to understand the potential synergistic effect of N and P in the flame-retardant effect, essays 15 and 16 were performed in absence of PA and urea respectively. It is clearly seen from PCFC results presented by [Fig. 5](#) that (1) urea alone (essay 15) exhibited a limited FR effect, (2) PA alone (essay 16) led to a strong decrease of HRR from 300.8 W/g for raw fiber to 72 W/g, (3) urea and PA have a synergistic effect resulting in the lower HRR value (42.9 W/g). In addition, it was observed that in the absence of urea (essay 16 compared to essay 13), the fiber produced retained significantly lower amounts of P (0.54 %) and was partially degraded and brittle, probably due to the highly acidic condition of the treatment. In essay 13, the presence of urea partially neutralized the acidity of the medium and prevented the fiber degradation.

The swelling behavior of the fibers was also evaluated by optical microscopy observations. Average fiber diameters were determined for dry untreated fiber (1), for fibers impregnated with water, fibers impregnated with a PA solution (conditions of essay 16) and with a

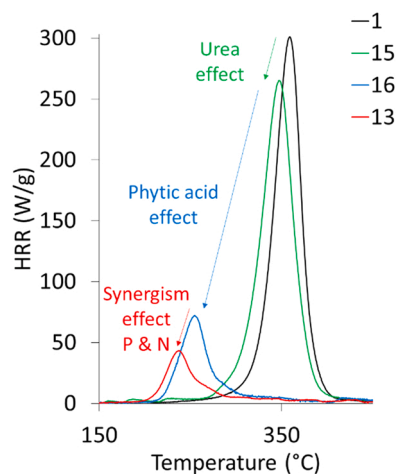
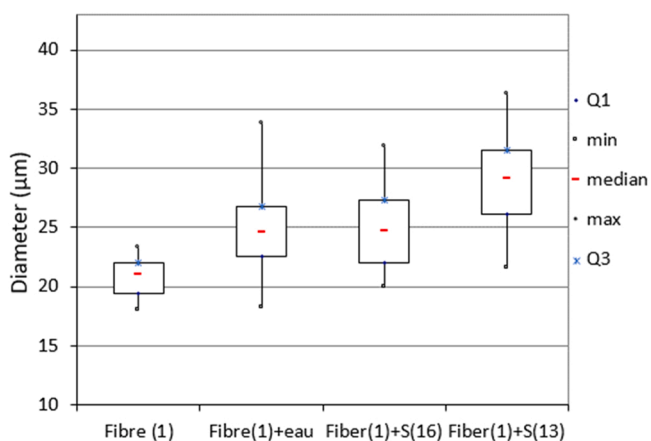


Fig. 5. HRR curves for fibers (1,15,16 and 13) in PCFC.

mixture urea/PA (essay 13). The results are presented in [Fig. 6](#) via box plots showing clearly a statistical observation which considers the values distributions of the 200 values. It can be seen that impregnation with water or PA led to a swelling of the fibers from a median diameter of  $\approx 22 \mu\text{m}$  to  $\approx 24\text{--}25 \mu\text{m}$  whereas a significantly larger swelling was observed in the presence of urea to reach a median diameter of  $\approx 29 \mu\text{m}$ . The swelling effect of urea aqueous solutions is well-known for cellulosic



**Fig. 6.** Box plots of fiber diameter as measured by optical microscopy and exposed to different swelling conditions (Fiber (1): dried fiber, Fiber (1)+WS: water impregnation, Fiber(1)+S(16): impregnation with phytic acid solution similar to essay 16 conditions, Fiber(1)+S(13): impregnation with phytic acid / urea mixture similar to essay 13 conditions).

fibers and has been widely studied in the literature (Isobe et al., 2013). It has been reported that urea has no direct interactions with cellulose but promotes water penetration into the cellulose crystals. This swelling effect observed in the presence of urea can explain the higher P content as observed previously with urea/PA mixtures (essay 13 compared to essay 16). Indeed, the swelling of the fibers allows a better penetration of the phosphorous reagent inside the fiber.

In order to confirm the thermal grafting of PA onto cellulose, the phosphorylation process was performed without the cooking step (essay 17, Supplementary Material SM7). In these conditions, N% and P% are very low (0.05 % and 0.1 % respectively), most of urea and PA being removed during the final washing step. As a result, the flame-retardant properties of the produced fibers are very weak.

Three phosphorylated fibers (essays 4, 13, 14) were characterized by  $^{13}\text{C}$  and  $^{31}\text{P}$  solid state NMR. The  $^{13}\text{C}$  spectra (Fig. 7-A) showed signals typical for cellulosic fibers. The peaks between 58 and 68 ppm, 80–91 ppm and 101–109 ppm attested the presence of C6, C4 and C1 carbon atoms respectively (Focher et al., 2001). C-4 and C-6 atoms are known to show well-separated  $^{13}\text{C}$  signals for crystalline (89 ppm, C-4 and 65 ppm, C-6) and disordered (84 ppm, C-4 and 63 ppm, C-6)

cellulose (Atalla and VanderHart, 1999; Montanari et al., 2005). The crystallinity index of cellulose (CI) can be determined by solid-state NMR according to (Park et al., 2009) as the ratio between the crystalline C4 contribution and the total C4 integral. Fiber 4, bleached and containing only 0.12 % P, and fiber 13, not bleached but with a high P content of 1.83 %, have a CI of 12 and 19, respectively. Interestingly, no crystalline contribution was detected for fiber 14, which was bleached and shows 2.40 % P. This decrease of cellulose crystallinity could be explained by the joint action of bleaching and phosphorylation processes.

A weak  $^{13}\text{C}$  signal at 160 ppm is attributed to the residual urea carbonyl function associated with the cellulose (Kristensen et al., 2004). This signal justified the nitrogen content detected in the samples after grafting. The presence of a strong  $^{31}\text{P}$  signal (Fig. 7-B) after thorough washing steps confirmed the successful grafting of PA in samples 3, 13 and 14. Corresponding  $^{13}\text{C}$  spectra also contained a phytic acid small contribution at 134 ppm. The  $^{31}\text{P}$  main signal centered at 0 ppm, typical for phosphate esters bound to cellulose (Fiss et al., 2019; Granja et al., 2001) doesn't enable the distinction of different P atoms of the grafted PA (Fig. 8-A and D).  $^{31}\text{P}$  spectra of fibers 13 and 14 displayed an additional shoulder, spreading down  $-15$  ppm, a chemical shift typical for poly-phosphates which could be related to a partial thermal condensation of phosphate units during the cooking step of the process (Fig. 8-E) similar to what was previously observed in the literature (Ghanadpour et al., 2018; Rol et al., 2020). In our case, this condensation was detected for fibers 13 and 14 containing high P contents.

The reaction of phosphorous molecule with polysaccharides in presence of urea has been extensively studied in the literature using starch or cellulose and different phosphorylating agent including phosphoric acid. It is assumed that during this reaction various chemical groups are produced such as phytate ester (Fig. 8-A) produced by cellulose phosphorylation (primarily at C6 position), carbamoylated glucose through a thermal disproportionation of urea (Fig. 8-B), the latter reaction producing also ammonia, bonded to phosphate groups of PA (Fig. 8-C). The complexation between the amide group of a carbamate moiety (B) and phosphate group through a strong hydrogen bond (Fig. 8-D) was also reported. This carbamate-phosphoric acid strong interaction has been studied in detailed by different authors using urea/ $\text{H}_3\text{PO}_4$  adduct (Ghanadpour et al., 2015) and for the phosphorylation of starch (Passauer and Bender, 2017). Based on our  $^{31}\text{P}$  NMR results previously exposed the formation of phytic pyrophosphate moiety by thermal dehydration of phytic acid can be also proposed (Fig. 8-E).

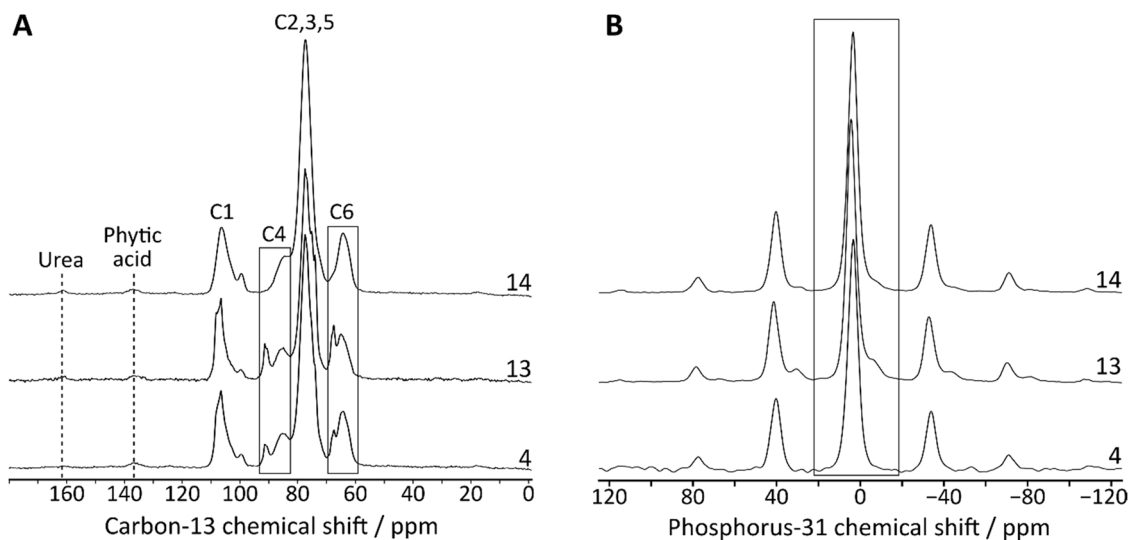


**Fig. 7.** Solid-state NMR spectra of fibers 4 (bottom), 13 (middle) and 14 (top). A:  $^{13}\text{C}$  CP spectra, where C atoms from cellulose are assigned. Boxes highlight cellulose C4 and C6 spectral regions, in which both amorphous and crystalline contributions can be distinguished (see text). B: quantitative  $^{31}\text{P}$  direct acquisition experiments: a box is drawn around the isotropic part of the spectrum; the peaks outside the box are spinning sidebands.

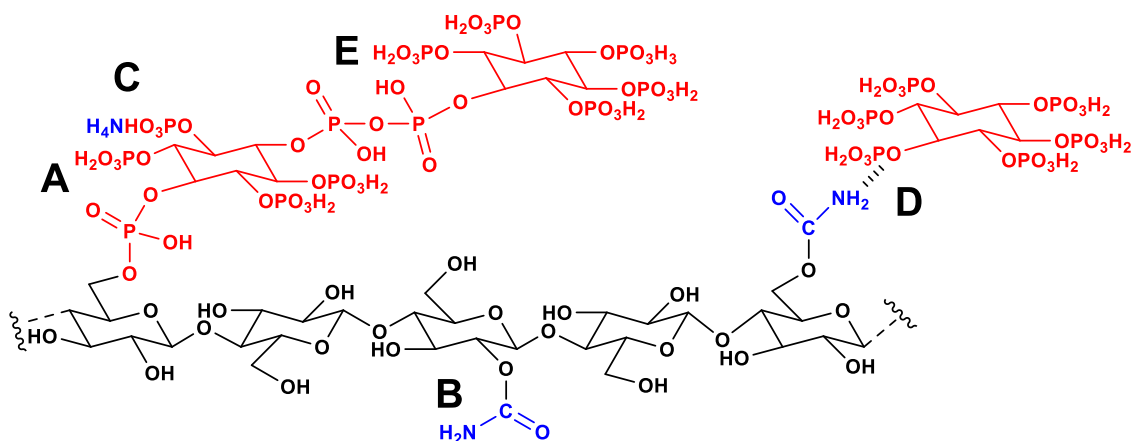


**Fig. 8.** Assumed phytic acid- cellulose derivatives: phytate ester (A), carbamate (B), ammonium phosphate (C), strong hydrogen bond (D) and phytic pyrophosphate (E).

The tensile properties of the raw HF (essay 1) and HF phosphorylated at two levels of process intensity (essay 9, P% = 0.93 % and essay 13, P% = 1.83 %) were analyzed in terms of tensile strength. It can be seen from Fig. 9 that the phosphorylation process has a significant impact on the mechanical properties of the resulting fibers. Under the conditions of essay 13, the median strength value of treated fibers drops significantly from 115 MPa to 20 MPa. The decrease in cellulose crystallinity observed by NMR and possible local damage induced by the treatment could explain the lower strength of phosphorylated fibers. It should be noted that by using the less severe phosphorylation conditions (essay 9), which use lower concentrations of PA and urea in the impregnation step, the mechanical properties of the fibers are less degraded with higher strength. The fibers from essay 9 are non-flammable (Fig. 9) and have a median strength of 75 MPa, 30 % lower than the untreated fiber.

#### 4. Conclusion

A solvent-free and environmentally friendly method has been optimized for natural fibers using phytic acid and urea as flame retardant. Phytic acid is a renewable and abundant phosphorylated flame retardant that can be isolated from the co-products of the oilseed industry. Non-flammable grafted fibers with low P and N content have been obtained through the P/N synergistic effect. The thermal stability and flammability of hemp fibers depend mainly on the phosphorous content. It was observed that a low phosphorous content improved the thermo-oxidative stability of char residue. However, a significant decrease in mechanical strength of 80 % was observed for grafted fibers with high phosphorous content due to a decrease in the crystallinity of the cellulose and possible local damage. An application of this work for the protection of wood and wood panels against fire will be reported later.

#### CRedit authorship contribution statement

**Karina Antoun:** Investigation, Conceptualization. **Melek Ayadi:** Investigation, Conceptualization. **Arnaud Besserer:** Methodology, Investigation, Analysis. **Rodolphe Sonnier:** Methodology, Investigation, Analysis. **Carole Gardiennet:** Methodology, Investigation, Analysis. **Michel Nahkl:** Project administration, Funding acquisition. **Roland El Hage:** Project administration, Supervision, Writing – original draft. **Nicolas Brosse:** Project administration, Supervision, Writing – original draft.

#### Declaration of Competing Interest

The authors declare that they have no known competing financial interests or personal relationships that could have appeared to influence

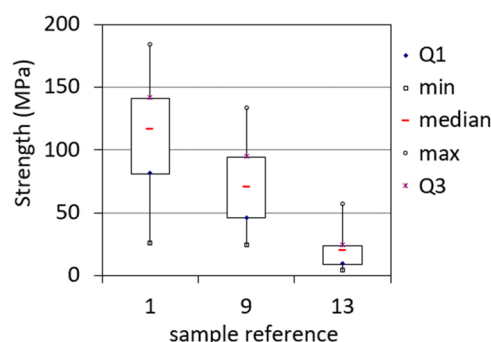


**Fig. 9.** Box plot of tensile properties of the raw fiber (essay 1) and non-bleached fibers phosphorylated at two levels of process intensity (essay 9 and essay 13).

the work reported in this paper.

#### Data Availability

No data was used for the research described in the article.

#### Acknowledgements

This work was also supported by the Lebanese University “Development and Innovation Project 2019–2021 (IGNABILOBAT)- Lebanon, EA 4370 LERMAB is supported by the French National Research Agency through the ARBRE Laboratory of Excellence (ANR-12-LABXARBRE-01), France. The authors thank the RMN platform, Institut Jean Barriol, CRM2, Université de Lorraine - CNRS, France, CETELOR, France (Centre d’Essais TEchnique LORrain, France) is acknowledged for supporting this research.

#### Appendix A. Supporting information

Supplementary data associated with this article can be found in the online version at [doi:10.1016/j.indcrop.2022.115265](https://doi.org/10.1016/j.indcrop.2022.115265).

#### References

- Alkandari, S., Bhatti, M.E., Aldughpassi, A., Al-Hassawi, F., Al-Foudari, M., Sidhu, J.S., 2021. Development of functional foods using psyllium husk and wheat bran fractions: Phytic acid contents. *Saudi J. Biol. Sci.* <https://doi.org/10.1016/j.sjbs.2021.03.037>.



- Atalla, R.H., VanderHart, D.L., 1999. The role of solid state  $^{13}\text{C}$  NMR spectroscopy in studies of the nature of native celluloses. *Solid State Nucl. Magn. Reson.* 15 (1), 1–19. [https://doi.org/10.1016/S0926-2040\(99\)00042-9](https://doi.org/10.1016/S0926-2040(99)00042-9).
- Chapple, S., Anandjiwala, R., 2010. Flammability of natural fiber-reinforced composites and strategies for fire retardancy: a review. *J. Thermoplast. Compos. Mater.* 23 (6), 871–893 <https://doi.org/10.1177/107092705709356338>.
- Coleman, R.J., Lawrie, G., Lambert, L.K., Whittaker, M., Jack, K.S., Grøndahl, L., 2011. Phosphorylation of alginate: synthesis, characterization, and evaluation of in vitro mineralization capacity. *Biomacromolecules* 12 (4), 889–897. <https://doi.org/10.1021/bm1011773>.
- Costes, L., Laoutid, F., Brohez, S., Dubois, P., 2017. Bio-based flame retardants: when nature meets fire protection. *Mater. Sci. Eng.: R: Rep.* 117, 1–25. <https://doi.org/10.1016/j.mser.2017.04.001>.
- Fiss, B.G., Hatherly, L., Stein, R.S., Friščić, T., Moores, A., 2019. Mechanochemical phosphorylation of polymers and synthesis of flame-retardant cellulose nanocrystals. *ACS Sustain. Chem. Eng.* 7 (8), 7951–7959. <https://doi.org/10.1021/acssuschemeng.9b00764>.
- Focher, B., Palma, M.T., Canetti, M., Torri, G., Cosentino, C., Gastaldi, G., 2001. Structural differences between non-wood plant celluloses: evidence from solid state NMR, vibrational spectroscopy and X-ray diffractometry. *Ind. Crops Prod.* 13 (3), 193–208. [https://doi.org/10.1016/S0926-6690\(00\)00077-7](https://doi.org/10.1016/S0926-6690(00)00077-7).
- Fung, B.M., Khitrin, A.K., Ermolaev, K., 2000. An improved broadband decoupling sequence for liquid crystals and solids. *J. Magn. Reson.* 142 (1), 97–101. <https://doi.org/10.1006/jmre.1999.1896>.
- García-Estapa, R.M., Guerra-Hernández, E., García-Villanova, B., 1999. Phytic acid content in milled cereal products and breads. *Food Res. Int.* 32 (3), 217–221. [https://doi.org/10.1016/S0963-9969\(99\)00092-7](https://doi.org/10.1016/S0963-9969(99)00092-7).
- Ghanadpour, M., Carosio, F., Larsson, P.T., Wågberg, L., 2015. Phosphorylated cellulose nanofibrils: a renewable nanomaterial for the preparation of intrinsically flame-retardant materials. *Biomacromolecules* 16 (10), 3399–3410. <https://doi.org/10.1021/acs.biomac.5b01117>.
- Ghanadpour, M., Wicklein, B., Carosio, F., Wågberg, L., 2018. All-natural and highly flame-resistant freeze-cast foams based on phosphorylated cellulose nanofibrils. *Nanoscale* 10 (8), 4085–4095. <https://doi.org/10.1039/C7NR09243A>.
- Granja, P.L., Pouysegou, L., Petraud, M., De Jeso, B., Baquey, C., Barbosa, M.A., 2001. Cellulose phosphates as biomaterials. I. Synthesis and characterization of highly phosphorylated cellulose gels. *J. Appl. Polym. Sci.* 82 (13), 3341–3353. <https://doi.org/10.1002/app.2193>.
- Hajj, R., El Hage, R., Sonnier, R., Otazaghine, B., Gallard, B., Rouif, S., Nakhil, M., Lopez-Cuesta, J.M., 2018. Grafting of phosphorous flame retardants on flax fabrics: Comparison between two routes. *Polym. Degrad. Stab.* 147, 25–34. <https://doi.org/10.1016/j.polymdegradstab.2017.11.006>.
- Hajj, R., El Hage, R., Sonnier, R., Otazaghine, B., Rouif, S., Nakhil, M., Lopez-Cuesta, J.M., 2020. Influence of lignocellulosic substrate and phosphorous flame-retardant type on grafting yield and flame retardancy. *React. Funct. Polym.* 153, 104612 <https://doi.org/10.1016/j.reactfunctpolym.2020.104612>.
- Huggett, Clayton, 1980. Estimation of rate of heat release by means of oxygen consumption measurements. *Fire Mater.* 4 (2), 61–65. <https://doi.org/10.1002/fam.810040202>.
- Hurrell, R.F., 2003. Influence of vegetable protein sources on trace element and mineral bioavailability. *J. Nutr.* 133 (9), 2973S–2977S. <https://doi.org/10.1093/jn/133.9.2973S>.
- Isobe, N., Noguchi, K., Nishiyama, Y., Kimura, S., Wada, M., Kuga, S., 2013. Role of urea in alkaline dissolution of cellulose. *Cellulose* 20 (1), 97–103. <https://doi.org/10.1007/s10570-012-9800-7>.
- Kristensen, J.H., Bampos, N., Duer, M., 2004. Solid state  $^{13}\text{C}$  CP MAS NMR study of molecular motions and interactions of urea adsorbed on cotton cellulose. *Phys. Chem. Chem. Phys.* 6 (12), 3175–3183. <https://doi.org/10.1039/B403537B>.
- Laufer, G., Kirkland, C., Morgan, A.B., Grunlan, J.C., 2012. Intumescent multilayer nanocoating, made with renewable polyelectrolytes, for flame-retardant cotton. *Biomacromolecules* 13 (9), 2843–2848. <https://doi.org/10.1021/bm300873b>.
- Li, J., Jiang, W., 2021. Synthesis of a novel PN flame retardant for preparing flame retardant and durable cotton fabric. *Ind. Crops Prod.* 174, 114205 <https://doi.org/10.1016/j.indcrop.2021.114205>.
- Liu, X.H., Zhang, Q.Y., Cheng, B.W., Ren, Y.L., Zhang, Y.G., Ding, C., 2018. Durable flame-retardant cellulosic fibers modified with novel, facile and efficient phytic acid-based finishing agent. *Cellulose* 25 (1), 799–811. <https://doi.org/10.1007/s10570-017-1550-0>.
- Lott, J.N., West, M.M., Clark, B., Beecroft, P., 1995. Changes in the composition of globoids in castor bean cotyledons and endosperm during early seedling growth with and without complete mineral nutrients. *Seed Sci. Res.* 5 (2), 121–125. <https://doi.org/10.1017/S0960258500002701>.
- Mandizvo, T., Odindo, A.O., 2019. Seed mineral reserves and vigour of Bambara groundnut (*Vigna subterranea* L.) landraces differing in seed coat colour. *Heliyon* 5 (5), e01635. <https://doi.org/10.1016/j.heliyon.2019.e01635>.
- Massiot, D., Fayon, F., Capron, M., King, I., Le Calvé, S., Alonso, B., Durand, J.O., Bujoli, B., Gan, Z., Hoatson, G., 2002. Modelling one- and two-dimensional solid-state NMR spectra. *Magn. Reson. Chem.* 40 (1), 70–76. <https://doi.org/10.1002/mrc.984>.
- Montanari, S., Roumani, M., Heux, L., Vignon, M.R., 2005. Topochemistry of carboxylated cellulose nanocrystals resulting from TEMPO-mediated oxidation. *Macromolecules* 38 (5), 1665–1671. <https://doi.org/10.1021/ma048396c>.
- Morgan, A.B., Gilman, J.W., 2013. An overview of flame retardancy of polymeric materials: application, technology, and future directions. *Fire Mater.* 37 (4), 259–279. <https://doi.org/10.1002/fam.2128>.
- Moussa, M., El Hage, R., Sonnier, R., Chrusciel, L., Ziegler-Devlin, I., Brosse, N., 2020. Toward the cottonization of hemp fibers by steam explosion. Flame-retardant fibers. *Ind. Crops Prod.* 151, 112242 <https://doi.org/10.1016/j.indcrop.2020.112242>.
- Park, S., Johnson, D.K., Ishizawa, C.I., Parilla, P.A., Davis, M.F., 2009. Measuring the crystallinity index of cellulose by solid state  $^{13}\text{C}$  nuclear magnetic resonance. *Cellulose* 16 (4), 641–647. <https://doi.org/10.1007/s10570-009-9321-1>.
- Passauer, L., Bender, H., 2017. Functional group analysis of starches reacted with urea-phosphoric acid-correlation of wet chemical measures with FT Raman spectroscopy. *Carbohydr. Polym.* 168, 356–364. <https://doi.org/10.1016/j.carbpol.2017.03.094>.
- Rol, F., Sillard, C., Bardet, M., Yarava, J.R., Emsley, L., Gablin, C., Léonard, D., Belgacem, N., Bras, J., 2020. Cellulose phosphorylation comparison and analysis of phosphate position on cellulose fibers. *Carbohydr. Polym.* 229, 115294 <https://doi.org/10.1016/j.carbpol.2019.115294>.
- Sauvageon, T., Lavoie, J.M., Segovia, C., Brosse, N., 2018. Toward the cottonization of hemp fibers by steam explosion—Part 1: defibrillation and morphological characterization. *Text. Res. J.* 88 (9), 1047–1055 <https://doi.org/10.1177/002040517517697644>.
- Sonnier, R., Otazaghine, B., Viretto, A., Apolinario, G., Lenny, P., 2015. Improving the flame retardancy of flax fabrics by radiation grafting of phosphorous compounds. *Eur. Polym. J.* 68, 313–325. <https://doi.org/10.1016/j.eurpolymj.2015.05.005>.
- Sykam, K., Försth, M., Sas, G., Restás, Á., Das, O., 2021. Phytic acid: a bio-based flame retardant for cotton and wool fabrics. *Ind. Crops Prod.* 164, 113349 <https://doi.org/10.1016/j.indcrop.2021.113349>.
- Van Meerten, S.G.J., Franssen, W.M.J., Kentgens, A.P.M., 2019. ssNake: a cross-platform open-source NMR data processing and fitting application. *J. Magn. Reson.* 301, 56–66. <https://doi.org/10.1016/j.jmr.2019.02.006>.
- Wan, C., Liu, M., Tian, P., et al., 2020. Renewable vitamin B5 reactive N–P flame retardant endows cotton with excellent fire resistance and durability. *Cellulose* vol. 27 (3), 1745–1761. <https://doi.org/10.1007/s10570-019-02886-z>.
- Wang, K., Meng, D., Wang, S., Sun, J., Li, H., Gu, X., Zhang, S., 2022. Impregnation of phytic acid into the delignified wood to realize excellent flame retardant. *Ind. Crops Prod.* 176, 114364 <https://doi.org/10.1016/j.indcrop.2021.114364>.
- Zhao, X., Liang, Z., Huang, Y., Hai, Y., Zhong, X., Xiao, S., Jiang, S., 2021. Influence of phytic acid on flame retardancy and adhesion performance enhancement of poly(vinyl alcohol) hydrogel coating to wood substrate. *Prog. Org. Coat.* 161, 106453 <https://doi.org/10.1016/j.porgcoat.2021.106453>.
- Ziegler-Devlin, I., Chrusciel, L., Brosse, N., 2021. Steam explosion pretreatment of lignocellulosic biomass: a mini-review of theoretical and experimental approaches. *Front. Chem.* 9 <https://dx.doi.org/10.3389/fchem.2021.705358>.